

文章编号: 2095-4980(2018)03-0558-07

Analysis and optimization of distance measurement in MATLAB/SIMULINK model

WANG Yin, JIN Xiangliang

(School of Physics and Optoelectronics, Xiangtan University, Xiangtan 411105, China and Hunan Engineering Laboratory for Microelectronics, Optoelectronics and System on a Chip, Xiangtan Hunan 411105, China)

Abstract: Based on the basic principle of Time-Of-Flight cameras, a novel MATLAB/SIMULINK model is proposed to measure phase delay of a modulated light signal which represents the distance from camera to object. Subsequently, by discussing influence factors of phase measurement, it is found that the integration time, the sampling time, and the aliasing effect have important effect on improving the accuracy of phase measurement. Interestingly, by analyzing different integration time and sampling time, it is found that the best integration time and sampling time are 0.05 ms and 10 ns, respectively. In this case(i.e.,in absence of the aliasing effect), the variation range of the distance error is between 1 mm and 11 mm in the interval of one period. Especially, under the consideration of the aliasing effect, the average value of distance error is half of that in absence of the aliasing effect. This improves the accuracy of the distance measurement greatly.

Keywords: Time-Of-Flight; pseudo-four-phase-shift algorithm; MATLAB/SIMULINK model; phase measurement

CLC number: TN249

Document code: A

doi: 10.11805/TKYDA201803.0558

1 Introduction

In recent years, great improvements are made in the field of optical distance measurement. Nowadays, three-dimensional(3D) matrix cameras can be used for many applications such as robotic, automotive, industrial, medical and multimedia^[1-4]. Up to now, there are three methods mainly utilized to acquire 3D information: stereo vision systems, laser range scanners and Time-Of-Flight(TOF) cameras^[5-9]. Stereo vision systems can provide high resolution images, texture and color information not just 3D geometry. Still, the major disadvantages of stereo vision systems are the limited field of view and the correspondence problem. Comparing to stereo vision systems, the range of laser range scanners is longer, so it is utilized to navigation tasks. However, the laser range scanner has its properties of a heavy weight, high power consumption and expensive prices, and it does not deliver two-dimensional(2D) intensity images and range data at the same time. To our surprise, TOF cameras can provide a 2D image of intensity and exact distance values in real-time. Compared with stereo vision systems, TOF cameras can deal with prominent parts of rooms such as walls, floors, and ceilings, even if they are not structured. Thereby, the TOF cameras become more and more attractive to a growing research community.

The basic problem of TOF cameras is the realization of a high accuracy of time measurement^[10-11]. For the distance measurement, ones are adopted to apply a continuous wave modulation. By far, for this distance measurement, there are two general methods. One is measuring phase difference between sent and received signals of the continuous wave modulation, and the other is measuring a light pulse's turn-around time. For the phase difference measurement method, only if the modulation frequency is known, will this measured phase directly correspond to the time of flight. In recent years, one main consideration is the accuracy of distance measurement. By considering external factors, Sun etc.^[12] designed a SIMULINK model of Phase-Shift Laser Rangefinder. They found that when some factors, such as the phase noise, the same frequency interference, the harmonic wave noise and so on, are considered, the accuracy of the distance

Received date: 2016-12-21; **Revised date:** 2017-03-18

Foundation: National Natural Science Foundation of China(61274043; 61233010); Hunan Provincial Natural Science Fund for Distinguished Young Scholars (2015JJ1014)

measurement is increased greatly. In order to improve measurement accuracy, Pu etc.^[13] compare two methods of the data processing in the distance measurement system. One method is first to calculate the average of four-road Fast Fourier Transform(FFT) value, and then to get the average values of FFT. The other is first to calculate each phase of the four-way FFT respectively, and then to obtain weighted sum of each phase. By comparing the two methods, they found that the accuracy of the distance measurement of the former is higher than that of the latter. In addition, ones also try to improve the algorithm of the distance measurement. Wang etc.^[14] studied the properties of the phase demodulation by the cosine signal phase spectrum analysis. It is shown that all phase spectrum analysis is suitable for high precision Phase-Shift Laser Rangefinder, and its precision degree is higher than that of the traditional Fourier method. Lin etc.^[15] also designed a simulation of the phase characteristics of hyperbolic sine function. They found that the fault location for HV transmission line can be detected on the noise based on phase ranging principle.

To our knowledge, a four-phase-shift algorithm is an effective distance measurement method. For a four-phase-shift algorithm, the optical signal is split into four equal interval sections in per period. The corresponding sampling points permit the unique determination of all relevant parameters of the incoming optical echo's waveform. The corresponding sampling points are acquired to sum over several hundreds or thousands of periods in an integration time, so that considerably increase the measurement accuracy. Furthermore, in order to decrease its system error and random error in the process of the distance measurement, Hussmann etc.^[16-20] use a pseudo-four-phase-shift algorithm to improve the accuracy. So, we here propose a novel SIMULINK model to achieve phase shift, by using pseudo-four-phase-shift algorithm. At the same time, we also optimize the sampling time of phase measurement and suppress the aliasing effect. Finally, it is found that the accuracy of phase measurement is improved.

This paper is structured as follows. In section II, we present TOF cameras of the distance measurement by the realization of the phase measurement. In section III, we propose 3D TOF SIMULINK model based on the pseudo-four-phase-shift algorithm. Subsequently, this model is applied to optimize the parameters of the influence phase error and to suppress the aliasing effect. It is found that the accuracy of distance measurement is improved. In the last section, brief conclusions are provided.

2 Real Time Processing of TOF Cameras

The TOF cameras make use of sensors to measure distance from camera to object with the illuminated scene. When a modulated optical signal is emitted by light-emitting diode to an object, and then is reflected by the object to camera system, the interval from emitting to receiving the optical signal can be recorded by detector. The phase difference between the emitted and the received optical echo is $\psi = \omega T_L$, here $\omega = 2\pi f_{\text{mod}}$ is the modulation frequency and T_L is TOF. The interval causes phase delay, which determines the distance maps from the camera to the object. The relation between the distance R and phase difference ψ is^[17]

$$R = \frac{c}{2f_{\text{mod}}} \left(\frac{\psi}{360^\circ} - N \right), \text{ with } N=0, 1, 2, 3 \dots \quad (1)$$

Here c represents the speed of light($3 \times 10^8 \text{ m} \cdot \text{s}^{-1}$), and f_{mod} is the modulation frequency of TOF cameras systems (in general, to our knowledge, $f_{\text{mod}}=20 \text{ MHz}$). N represents the ambiguity in range estimation when $\psi > N \cdot 360^\circ$. Hence, when the TOF cameras implement a complete phase map, the distance maps can be acquired.

In order to obtain the phase delay of a modulated optical signal, we here introduce the principle of phase measurement. Based on that the received optical signal amplitude a depends on the reflectivity coefficient, the phase ψ would be synchronously demodulated within the detector. Considering that the received signal is mostly superimposed on the received average incident light(background light and digital camera component of the modulated light source), we add an offset B to obtain the real measured value. The optical signal can be described as^[17]

$$P_{\text{opt}}(t - \psi) = a \cos(\omega t - \psi) + B \quad (2)$$

To acquire the phase difference ψ , we also offer the same frequency of square wave signal. The square wave signal $g(t)$ can be given by

$$g(t) = \sum_{n=-\infty}^{\infty} \text{rect}(\omega t - n \cdot 2\pi) = \frac{2}{\pi} \left[\cos(\omega t) - \frac{1}{3} \cos(3\omega t) + \frac{1}{5} \cos(5\omega t) - \dots \right] \quad (3)$$

The square wave is made up of several odd harmonics. Demodulation of the received optical signal can be performed by correlation with the square wave modulation signal based on the cross correlation of process. The correlation function $\phi(\tau)$ is defined as

$$\begin{aligned} \phi(\tau) &= P_{\text{opt}}(\tau + t - \psi) \otimes g(t) = \lim_{T \rightarrow \infty} \frac{1}{T} \int_{-\frac{T}{2}}^{\frac{T}{2}} P_{\text{opt}}(\tau + t - \psi) \cdot \sum_{n=-\infty}^{\infty} \text{rect}(\omega t - n \cdot 2\pi) dt = \\ & \lim_{T \rightarrow \infty} \frac{1}{T} \int_{-\frac{T}{4}}^{\frac{T}{4}} P_{\text{opt}}(\tau + t - \psi) dt = \frac{a}{\pi} \cos(\omega\tau - \psi) + \frac{B}{2} \end{aligned} \quad (4)$$

Here T represents one periodic time. From the Equation (2), one can see that the amplitude and the received average incident light have an effect on the phase measurement. So, we here apply the four phase-shift algorithm to measure phase. And we set four different phases as $\omega\tau = 0^\circ, 90^\circ, 180^\circ$, and 270° . Correspondingly, the four phases respectively are $\phi(0^\circ) = a \cos \psi / \pi + B/2$, $\phi(90^\circ) = -a \sin \psi / \pi + B/2$, $\phi(180^\circ) = -a \cos \psi / \pi + B/2$, and $\phi(270^\circ) = a \sin \psi / \pi + B/2$. By decreasing the optical echo's amplitude and the received average incident light, we obtain that the phase ψ and amplitude A is

$$\psi = \arctan \left(\frac{\phi_{270^\circ} - \phi_{90^\circ}}{\phi_{0^\circ} - \phi_{180^\circ}} \right) \quad (5)$$

$$A = \frac{\delta}{\Delta t \sin \delta} \cdot \frac{\sqrt{[\phi_{270^\circ} - \phi_{90^\circ}]^2 + [\phi_{0^\circ} - \phi_{180^\circ}]^2}}{2} \quad (6)$$

The measured amplitude is attenuated by a factor of $\delta / (\Delta t \cdot \sin \delta)$ depending on the sampling time Δt , with $\delta = \pi \Delta t / T$. When the received signal is split into four sections, each section possesses own message of the received average incident light. So, by decreasing the optical echo's amplitude, the received average incident lights have two types which can be described as

$$B_1 = \phi_{0^\circ} + \phi_{180^\circ} \quad (7)$$

and

$$B_2 = \phi_{90^\circ} + \phi_{270^\circ} \quad (8)$$

3 MATLAB/SIMULINK Blocks Mode of Phase Measurement

On the basis of pseudo-four-phase-shift algorithm, we propose a SIMULINK model to measure and calculate phase. This model is utilized to optimize the influence parameters of phase measurement and to suppress the aliasing effect. Finally, the accuracy of phase measurement is improved. The SIMULINK block diagram of a complete drive system is presented in Fig.1. For example, the sine wave block corresponds to a received signal, of which the frequency, phase, and bias are 20 MHz, $\pi/2$, and 1, respectively. The pulse generator block is a modulation signal of the same frequency as a received signal. Time delay block represents the time of flight in the system. Based on the four phase-shift algorithm, we set four different phases as $\omega\tau = 0^\circ, 90^\circ, 180^\circ$, and 270° , which are input in the Delay 0, Delay 2, Delay 1, and Delay 3 blocks, respectively. Product blocks act as a modulating part by the modulating signal multiplied by the received signal. Integrator blocks implement a typical integration time. Add and Add 1 blocks deal with arithmetic operation of $\phi_{0^\circ} - \phi_{180^\circ}$ and $\phi_{270^\circ} - \phi_{90^\circ}$ in the Equation(5), respectively. Subsequently, the data of $\phi_{0^\circ} - \phi_{180^\circ}$ and $\phi_{270^\circ} - \phi_{90^\circ}$ are read out by Scope and Scope 1

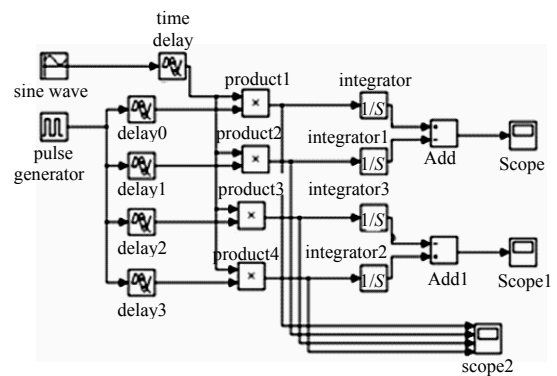


Fig.1 MATLAB/SIMULINK block mode of the phase measurement

blocks, respectively. These data will be utilized to calculate the phase shift in the SIMULINK workplace. The Scope 2 block is a testing availability of four-phase-shift algorithm.

Based on demodulation and sampling principle, the received optical signal is split into four equal sampling time periods Δt in the range of one periodic time^[11]. Fig.2 shows the demodulation signal of the received signal of the Scope 2 block in the Fig.1. We find that with the increasing integration time T_{int} (integration time), the amplitudes of cosine function exhibit different curves with different phases. For each sampling time, the area, which is surrounded by the curves of the amplitude and the horizontal ordinate, is expressed by $a_i(i=0,1,2,3)$ that is generally called the sampling point. We also find that the curves of all sampling point appear zigzag shape. For each sampling point, by accumulating over several hundreds or thousands of periods, we obtain integrated values A_i (i.e., $A_i = \sum a_i$), which will increase the signal to noise ratio and the accuracy of the measurement.

The accuracy of the phase measurement is relative with the integration time. From Fig.2, it is seen that the integration time is a series of cyclical discrete sampling time. Theoretically, the integration time is just expressed by the equation(4). And the result of the convolution function in the equation(4) is an invariable value within a period. For the longer time, the correlation function $\phi(\tau)$ can be described as

$$\phi(\tau) = P_{opt}(\tau + t - \psi) \otimes g(t) = \lim_{T \rightarrow \infty} \frac{1}{T} \int_0^{\beta/\omega} P_{opt}(\tau + t - \psi) g(t) dt = \frac{a}{2\pi} \left[\sin \frac{\beta}{2} \cos(\omega\tau - \psi) + \cos \frac{\beta}{2} \sin(\omega\tau - \psi) \right] + \frac{\beta}{4\pi} B \quad (9)$$

Here, β/ω is just the integration time. If the sampling point of the equation(4) is satisfied, namely, the sampling point is $a \cos(\omega\tau - \Psi)/2\pi + B/4$, it is obtained that $\beta = \pi$. When the sampling point is $-a \sin(\omega\tau - \Psi)/2\pi + B/2$, we obtain that $\beta = 2\pi$. By such analogy, we can conclude that $\beta = k\pi$, with $k=1,2,3 \dots$. That means the integration time is the integer multiples of the half of the period time, namely, $T_{int} = kT/2$, with $k=1, 2, 3 \dots$. However, the integration time is longer, and the speed of simulation's data transmission is slower. Thereby, in order to obtain the best operation time, we here choose the phase shift 60° as a typical example. When the phase shift 60° is input into the 3D model, the simulating data change with the integration time as shown in Fig.3. It is shown that the simulating data tends to be stable within the interval of about 1.0×10^{-6} s and then approaches to the real phase 60° . It illustrates that the stable interval of the four sampling data is beyond one period (which is 50 ns) at least. As above mentioned, $T_{int} = kT/2$, with $k=1, 2, 3 \dots$, and the period of our SIMULINK model is 50 ns, so that $T_{int} = 25k$ (ns) with $k=1, 2, 3 \dots$. From this result, combining with the stable point in the Fig.3, it is obtained that the best integration time in our SIMULINK block is 0.05 ms. Thereby, in the following calculation, we will accumulate 1 000 times over the sampling points to get an integrated value A_i .

In addition, the sampling time Δt also affects the accuracy of the phase measurement in the TOF system. As the discussion in the document [11], the sampling time $\Delta t = T/4$ of the equation(6) is decreased to 90% of the real amplitude. When $\Delta t = T/2$, the measured amplitude is 64% of the real amplitude. So, we here discuss the effect of

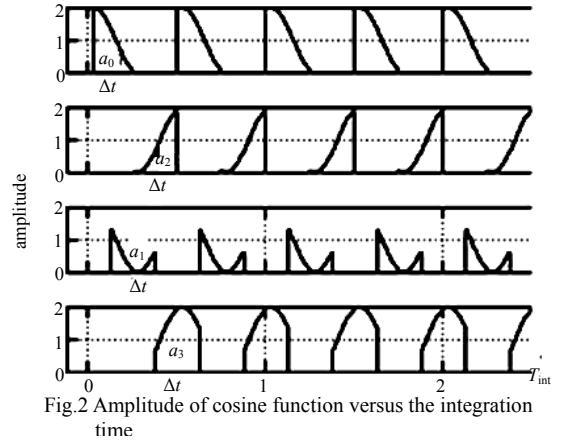


Fig.2 Amplitude of cosine function versus the integration time

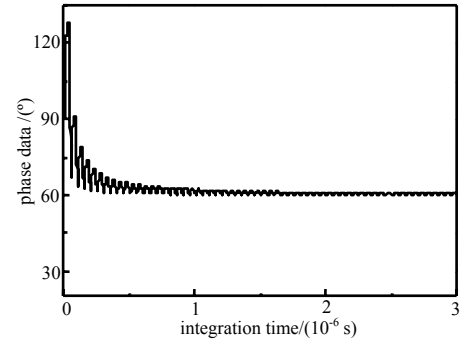


Fig.3 Phase data of input phase shift $\phi_i = 60^\circ$ into 3D model as a function of the integration time

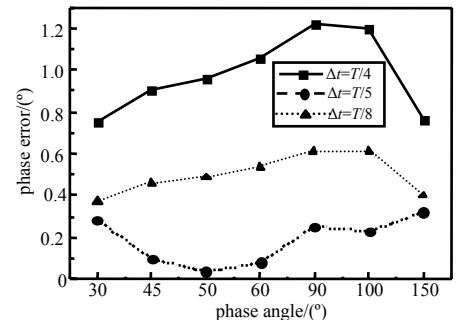


Fig.4 Phase error versus the input phase angle with different sampling time

the sampling time on the accuracy of the phase measurement. Due to that the sampling time must meet the condition of an integer number of the sampling points, we choose the sampling time as $\Delta t = T/4, T/5$, or $T/8$.

Fig.4 shows the phase error versus the input phase angle with different sampling time. When the sampling time is $\Delta t = T/4$, the range of the phase error is in 0.75 and 1.2. While $\Delta t = T/5$, the phase error is among 0.05 and 0.3. If $\Delta t = T/8$, the phase error is 0.35 and 0.6. Obviously, the sampling time $\Delta t = T/5$ satisfies the condition of the minimum error. From this, it can be concluded that the best sampling time is $\Delta t = 10$ ns. Therefore, we choose the sampling time as $\Delta t = 10$ ns in the following 3D TOF model simulation.

After both the integration time and sampling time are chosen, we further read the output data of $\phi 0^\circ - \phi 180^\circ$ and $\phi 270^\circ - \phi 90^\circ$ from scope and scope 1 block in the Fig.1. Subsequently, the output data of the $\phi 0^\circ - \phi 180^\circ$ and $\phi 270^\circ - \phi 90^\circ$ varying with the integration time are depicted in Fig.5. It is found that the value of the $\phi 0^\circ - \phi 180^\circ$ is bigger than that of the corresponding points of $\phi 270^\circ - \phi 90^\circ$. On the basis of the data of the Fig.5 and the four-phase-shift algorithm, when the input phase ϕ_1 is in the different range, the phase can be described as^[19]

$$\psi = 90^\circ - \arctan\left(\frac{\phi 270^\circ - \phi 90^\circ}{\phi 0^\circ - \phi 180^\circ}\right) \quad \text{if } 0^\circ \leq \phi_1 < 180^\circ \quad (10)$$

$$\psi = 270^\circ - \arctan\left(\frac{\phi 270^\circ - \phi 90^\circ}{\phi 0^\circ - \phi 180^\circ}\right) \quad \text{if } 180^\circ \leq \phi_1 < 360^\circ \quad (11)$$

From Equation(10) and Equation(11), we can acquire the simulation phase. Then, substituting the phase value into Equation (1), we can calculate the distance from cameras to object.

As matter of fact, when we input a phase of a cosine signal wave corresponding to the time of flight, we achieve the simulation data from our SIMULINK model by optimizing the integration time and sampling time. The deviation value of distance measurement is shown in Fig.6 based on TOF cameras principle. It is found that the variation range of the distance error is between 1 mm and 11 mm in the interval of one period. It is possible that the distance error is caused by the integration time and the sampling time in the model.

As above mentioned, the square wave is made up of several odd harmonics, and the curves of all sampling points in the Fig.2 appear zigzag shape. However, the asymmetric sawtooth wave will cause the phase error^[21]. As discussed in the document [11], if the sampling time is chosen as $\Delta t = T/2$, all even harmonics of the basic frequency, namely $2f, 4f, \dots$ will be suppressed and do not contribute to the demodulation result, while the optical signal is correlated with odd harmonics of the square wave frequency and will influence the demodulation result due to the aliasing effect. And the suppression of aliasing effect is relative with the sampling time. This simple example illustrates that the choice of the sampling time Δt is rather important for the demodulation result. In our SIMULINK model (see Fig.1), the demodulation signal is a square wave which can be split into a sum of odd harmonics of the fundamental frequency with decreasing amplitude for increasing frequency as shown in the Equation(3). Considering the sampling time of sampling points, $5f$ -harmonic is suppressed, while the other odd harmonics have influence on demodulation result.

Because the aliasing effect is independent of the signal amplitude, we regard it as an additive noise. In order to suppress the additive noise, we take criterion sine wave into account in our model. That is to say, the original input signal(which is shown as the Fig.7(a)) is replaced by a new criterion sine wave(it is shown in the Fig.7(b)). Accordingly, the output model of the original (the Fig.8(a)) is also replaced with that of a new Fig.8(b). In this case, the other parameters in our model are kept fixed. By the same processes, we obtain the simulation data of $\phi 0^\circ + \phi 180^\circ$ and $\phi 90^\circ + \phi 270^\circ$ from Scope and

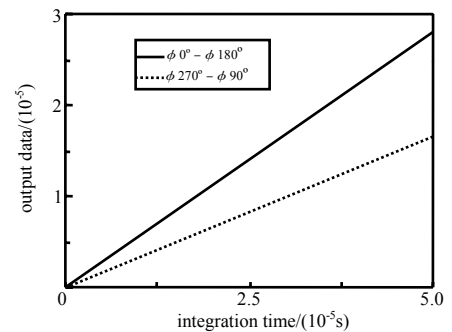


Fig.5 Output data of scope and scope 1 in the Fig.1 as a function of the integration time

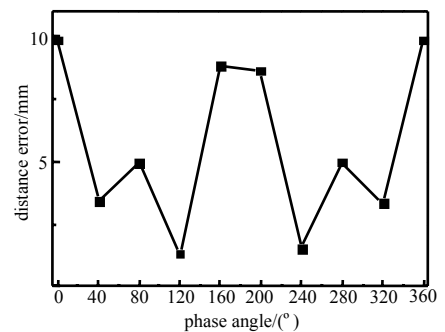


Fig.6 Distance error as a function of input phase angle

Scope1 in Fig.1, respectively. The value is expressed as the additive noise which is aliasing effect. After the consideration of aliasing effect, the phase expression of the pseudo-four-phase-shift algorithm is

$$\psi = \arctan\left(\frac{(\phi_{270^\circ} - \phi_{90^\circ}) + B_2}{(\phi_{0^\circ} - \phi_{180^\circ}) + B_1}\right) \quad (12)$$

Moreover, we input the phase to get their simulation data by means of Equation(12). And we can acquire a deviation value of distance measurement as shown in the dotted line of Fig.9. It is found that the variation range of the distance error is between 0 and 5 mm in the interval of one period. By comparing the solid line(which is just the curve of Fig.(6) and the dotted lines in the Fig.9, we find that the average value of distance error after considering the aliasing effect is half of that before considering the aliasing effect. Therefore, we conclude that the suppression of the aliasing effect can decrease the error value of the distance, and correspondingly improve the accuracy of distance measurement.

4 Conclusions

In summary, the distance from cameras to object can be calculated by the phase delay of a modulated light signal in the TOF camera systems. Subsequently, the measurement method of the phase delay is described based on four-phase-shift algorithm. We propose a novel MATLAB/SIMULINK model to measure phase delay of a modulated light signal which represents the distance from camera to object. In our model, a signal phase, which corresponds to time of light, is input and then is implemented in our SIMULINK model to get the data of the phase. By means of simulating the phase angle, it illustrates the availability of four-phase-shift algorithm. Meanwhile, it is found that the factors influencing the phase error are integration time, sampling time and aliasing effect. Then, by optimizing the integration time and the sampling time, we find that the best integration and sampling time are chosen as 0.05 ms and 10 ns, respectively. In this case, the variation range of the distance error is between 1mm and 11mm in the interval of one period. Thereby, we finally conclude that the aliasing effect will affect on the distance measurement. In order to suppress the aliasing effect, a criterion sine wave is taken into account. Corresponding output models are also replaced by a new operation symbol. Under the consideration of the aliasing effect, we find that the average value of distance error is half of that in absence of the aliasing effect.

References:

- [1] KANG H J, CHUN B J, JANG Y S, et al. Real-time compensation of the refractive index of air in distance measurement[J]. Optics Express, 2015, 23(20):26377–26385.
- [2] KAHLMANN T, INGENSAND H. Calibration and development for increased accuracy of 3D range imaging cameras[J]. Journal of Applied Geodesy, 2008, 2(1):1–11.
- [3] ZHOU P, BURGE J H. Optimal design of computer generated holograms to minimize sensitivity to fabrication errors[J]. Optics Express, 2007, 15(23):15410–15417.
- [4] GOKTURK S B, TOMASI C. 3D head tracking based on recognition and interpolation using a time-of-flight depth sensor[C]// Proceedings of the IEEE Conference on Computer Vision and Pattern Recognition. Washington, D C, USA: [s.n.], 2004:211–217.

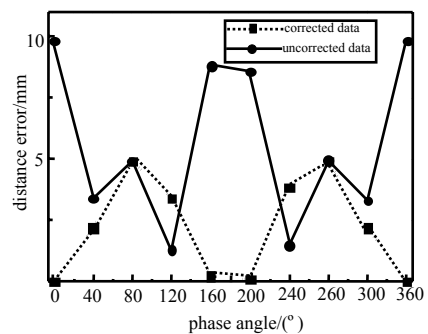
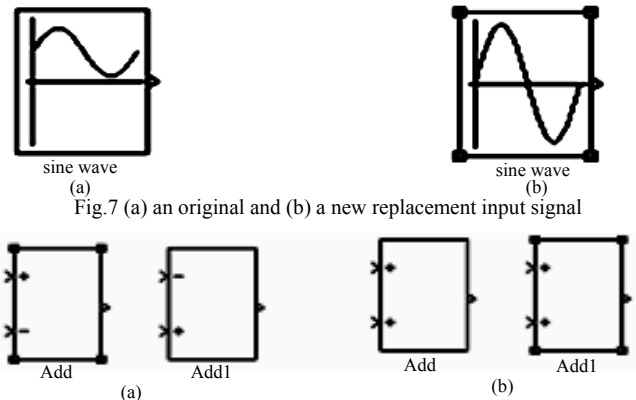


Fig.9 Distance error versus the input phase angle under the consideration of aliasing effect(dotted line) or not(solid line)

- [5] BARFOOT T,FURGALE P,STENNING B,et al. Field testing of a rover guidance, navigation, and control architecture to support a ground-ice prospecting mission to Mars[J]. *Robotics and Autonomous Systems*, 2011,59(6):472–488.
- [6] SCHWARTE R,XU Z,HEINOL H,et al. New electro-optical mixing and correlating sensor:facilities and applications of the photonic mixer device(PMD)[C]// *Lasers and Optics in Manufacturing III*. International Society for Optics and Photonics. [S.l.]:SPIE, 1997:245–253.
- [7] BLANC N,OGGIER T,GRUENER G,et al. Miniaturized smart cameras for 3D-imaging in real-time[C]// *Proc. of the IEEE Sensors*. [S.l.]:IEEE, 2004:471–474.
- [8] VASKEVICIUS N,BIRK A,PATHAK K,et al. Efficient representation in 3D environment modeling for planetary robotic exploration[J]. *Advanced Robotics*, 2010,24(8/9):1169–1197.
- [9] OGGIER T,LEHMANN M,KAUFMANN R,et al. An all-solid-state optical range camera for 3D real-time imaging with sub-centimeter depth resolution(SwissRanger)[C]// *Optical Design & Engineering*. [S.l.]:Proceedings SPIE, 2004:534–545.
- [10] LANGE R D,SEITZ P. Solid-state time-of-flight range camera[J]. *IEEE Journal of Quantum Electronics*, 2001(37):390–397.
- [11] LANGE R D. 3D time-of-flight distance measurement with custom solid-state image sensors in CMOS/CCD-technology[D]. Nordrhein-Westfalen:Siegen University, 2000.
- [12] 孙英,张珂殊. 相位式激光测距仿真系统的设计与实现[J]. *计算机仿真*, 2012,29(1):360–363. (SUN Y,ZHANG K S. Design and implementation of simulation system for phase-shift laser range finder[J]. *Computer Simulation*, 2012, 29(1):360–363.)
- [13] 蒲磊,刘恩海,钟建勇. 基于四象限APD相位法测距的数据融合各方法比较[J]. *半导体光电*, 2014,35(6):1075–1079. (PU L,LIU E H,ZHONG J Y. Comparison of data fusion methods of the phase ranging based on four-quadrant APD[J]. *Semiconductor Optoelectronics*, 2014,35(6):1075–1079.)
- [14] 王选钢,缙宁祎,张珂殊. 相位式激光测距全相位谱分析鉴相算法[J]. *太赫兹科学与电子信息学报*, 2012,10(6):725–729. (WANG X G,GOU N Y,ZHANG K S. ApFFT phase discrimination in phase-shift laser range finder[J]. *Journal of Terahertz Science and Electronic Information Technology*, 2012,10(6):725–729.)
- [15] 林富洪,王增平,李金龙,等. 基于双曲正弦函数相位特性高压故障线路相位测距[J]. *电力系统保护与控制*, 2010, 38(14):28–33. (LIN F H,WANG Z P,LI J L,et al. Fault location algorithm for HV transmission line based on phase characteristics of hyperbolic sine function[J]. *Power System Protection and Control*, 2010,38(14):28–33.)
- [16] HUSSMANN S,RINGBECK T,HAGEBEUKER B. A performance review of 3D TOF vision systems in comparison to stereo vision systems[M]. Vienna,Austria:I-Tech Education and Publishing, 2008.
- [17] HUSSMANN S,EDELER T. Performance improvement of a 3D-TOF PMD camera using a pseudo 4-phase shift algorithm[C]// *Instrumentation and Measurement Technology Conference*. [S.l.]:IEEE, 2009:542–546.
- [18] HUSSMANN S,EDELER T. Pseudo-four-phase-shift algorithm for performance enhancement of 3D-TOF vision systems[J]. *IEEE Transactions on Instrumentation & Measurement*, 2010,59(5):1175–1181.
- [19] HUSSMANN S,EDELER T,HERMANSKI A. Real-time processing of 3D-TOF data in machine vision applications[M]. Los Angeles,USA:InTech, 2012.
- [20] HUSSMANN S,LIEPERT T. 3D-TOF robot vision system[J]. *IEEE Transactions on Instrumentation and Measurement*, 2009,58(1): 141–146.
- [21] PAN H D. Research on mechanisms and characteristics of non-scanning time-of-flight 3D imaging camera[D]. Hangzhou,China: Zhejiang University, 2010.

About the authors :



WANG Yin(1988–), male, was born in Chenzhou, Hunan province. Master degree. The main research direction is electronic science and technology.email:rexlolo@163.com.

JIN Xiangliang(1974–), male, was born in Changsha, Doctor degree, professor. The main research direction is electronic engineering.